

Long-term responses to changes in Arctic soil hydrology

Félix García-Pereira¹, J. F. González-Rouco¹, N. Meabe-Yanguas¹, J. H. Jungclaus², P. De Vrese², and S. J. Lorenz²

¹Complutense University of Madrid (UCM) and Geosciences Institute (IGEO, UCM-CSIC), Madrid, Spain

²Max Planck Institute for Meteorology, Hamburg, Germany

Corresponding author: Félix García-Pereira (felgar03@ucm.es)



Abstract

Global warming induces temperature and water availability changes in the Arctic that affect the soil moisture and ice presence, and subsequently the soil thermal structure in permafrost regions. Notwithstanding, the interaction between soil hydrology and thermodynamics is still poorly represented by most of the CMIP6 land surface models (LSMs), mainly in terms of the soil depth, vertical resolution, and coupling between hydrology and thermodynamics. This work explores the response of the Max Planck Institute Earth System Model (MPI-ESM) to changes in the hydrological and thermodynamic features of its LSM, JSBACH, in permafrost active regions. A set of ongoing experiments covering the past2k (0-1850), the historical period (1850-2014), and different climate change scenarios (SSPs, 2015-2100) with variations in soil depth and vertical resolution under two hydro-thermodynamic coupling configurations was prepared. These set-ups generate comparatively drier (DRY) or wetter (WET) conditions in the Arctic, allowing for assessing climate responses and feedbacks when compared to the reference (REF) Arctic hydroclimate.

Results show that deepening JSBACH reduces the intensity of near-surface warming, reducing the deep permafrost degradation area by ca. 2 million km² and constraining the active layer thickness deepening by the end of the 21st century in high radiative forcing scenarios. Nevertheless, the largest impacts on permafrost extent and active layer thickness are produced by the different hydrological settings, which yield diverging soil moisture and warming conditions during the 21st century. The analysis of the past2k simulations will allow for assessing the regional and global influences of Arctic physics in a multi-centennial context.

1. The JSBACH-HTCp ensemble

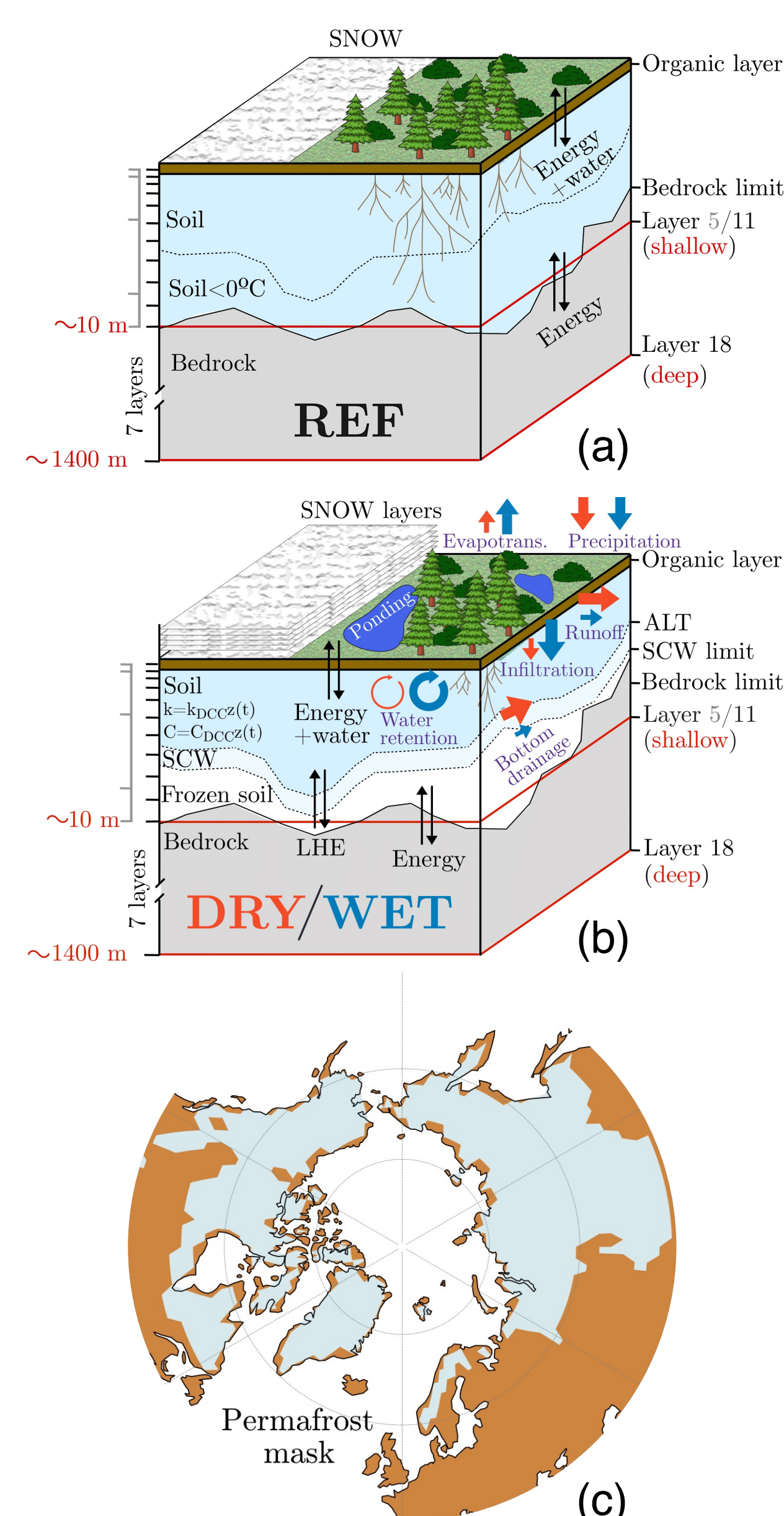


Fig. 1. HTCp thermo-hydrodynamical changes applied to JSBACH standard version (REF, a). (b) Conceptual sketch showing the features and the intensity (arrow thickness) of different thermodynamical and hydrological processes for DRY (red) and WET (blue) configurations with respect to REF. (c) Permafrost mask where the JSBACH-HTCp physics are implemented [1]. Outside the area portrayed by the permafrost mask in (c), the REF configuration of JSBACH is used.

The sensitivity of permafrost to changes in the standard JSBACH soil hydrology (REF, Fig. 1a) is assessed tuning some processes and parametrizations of the Arctic water-cycle, creating the **WET** and **DRY** configurations (Fig. 1b). These two configurations aim to represent two extreme hydrological states of the Arctic covering the range of uncertainty shown by CMIP6 models in future climate simulations. An ensemble of nine Pre-industrial control (PIC), historical (HIS, 1850-2014) and scenario (SSP, 2015-2100) simulations is conducted (Fig. 2) by combining the three configurations WET, DRY, and REF and the three LSM discretizations, with 5, 11, and 18 layers. For the 18-layer simulations, a prePIC phase of 100 years is run to speed up the thermal equilibrium of the subsurface temperature column.

2. Active layer thickness (ALT) response to HTCp changes

ALT spatial values are the smallest for WET (Fig. 3a). This is due to the relative colder regional temperatures compared to DRY simulations (Fig. 5). However, REF spatial median ALT is ca. 1 (2) m greater than DRY (WET) up to the first quarter of the 21st century, despite showing colder (similar) surface air and ground surface temperatures (Fig. 5a,b). Fig. 3b,c further shows ALT for REF is greater than for DRY for ca. 70 (60) % of the points in the 1850-1900 (2000-2014) period. **This overall overestimation of REF ALT is most likely due to the fact that the standard JSBACH does not include freezing-thawing processes, neglecting the "counterbalance" zero-curtain effect [7,8] in summer.**

Moreover, deepening JSBACH reduces ALT thickening with warming for the three HTCp configurations, preventing that ca. a 10 % of the permafrost points are completely thawed by 2085-2099 (Fig. 3e).

A modified version of JSBACH3.2 (Fig. 1a, [2]) allowing for hydro-thermodynamical soil coupling in permafrost regions in fully-coupled MPI-ESM simulations [3] is used in this work (JSBACH-HTCp; Fig. 1b). These changes are active only across the areas covered by the mask shown in Fig. 1c. They consist of the inclusion of a multi-layer snow scheme, the dynamical response of soil thermal properties to hydrological changes, the allowance of water phase changes within the soil (soil ice formation), an improved representation of the organic layer, and the inclusion of a wetland scheme [3,4]. Furthermore, the JSBACH3.2 standard discretization of 5 layers with a LSM depth of 9.83 m was deepened and refined near the surface. Thus, two new vertical layering schemes are introduced (Fig. 1a,b): a resolution-enhanced 11-layer scheme with a LSM depth of 9.83 m, and a deepened 18-layer scheme of 1391.48 m, which ensures the bottom layer thermal decoupling from ground surface conditions in multi-centennial timescales [5,6].

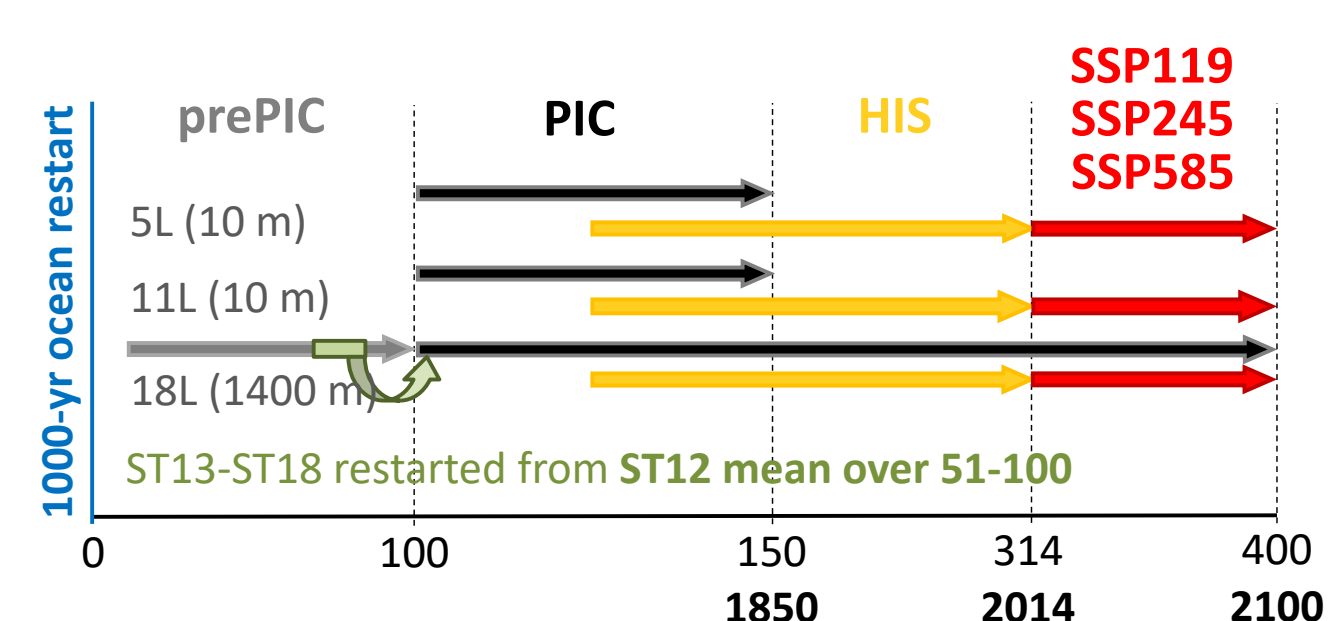


Fig. 2. Experimental setup of the MPI-ESM JSBACH-HTCp ensemble. Scheme of pre-industrial control (prePIC, grey; PIC, black), historical (HIS, yellow), and 21st century climate change Shared Socioeconomic Pathway forcing scenarios (SSP119, SSP245, and SSP585, red arrows) simulations for each of the three different JSBACH-HTCp configurations (DRY, WET, and REF; Fig. 1) and vertical discretizations (5, 11, and 18 layers).

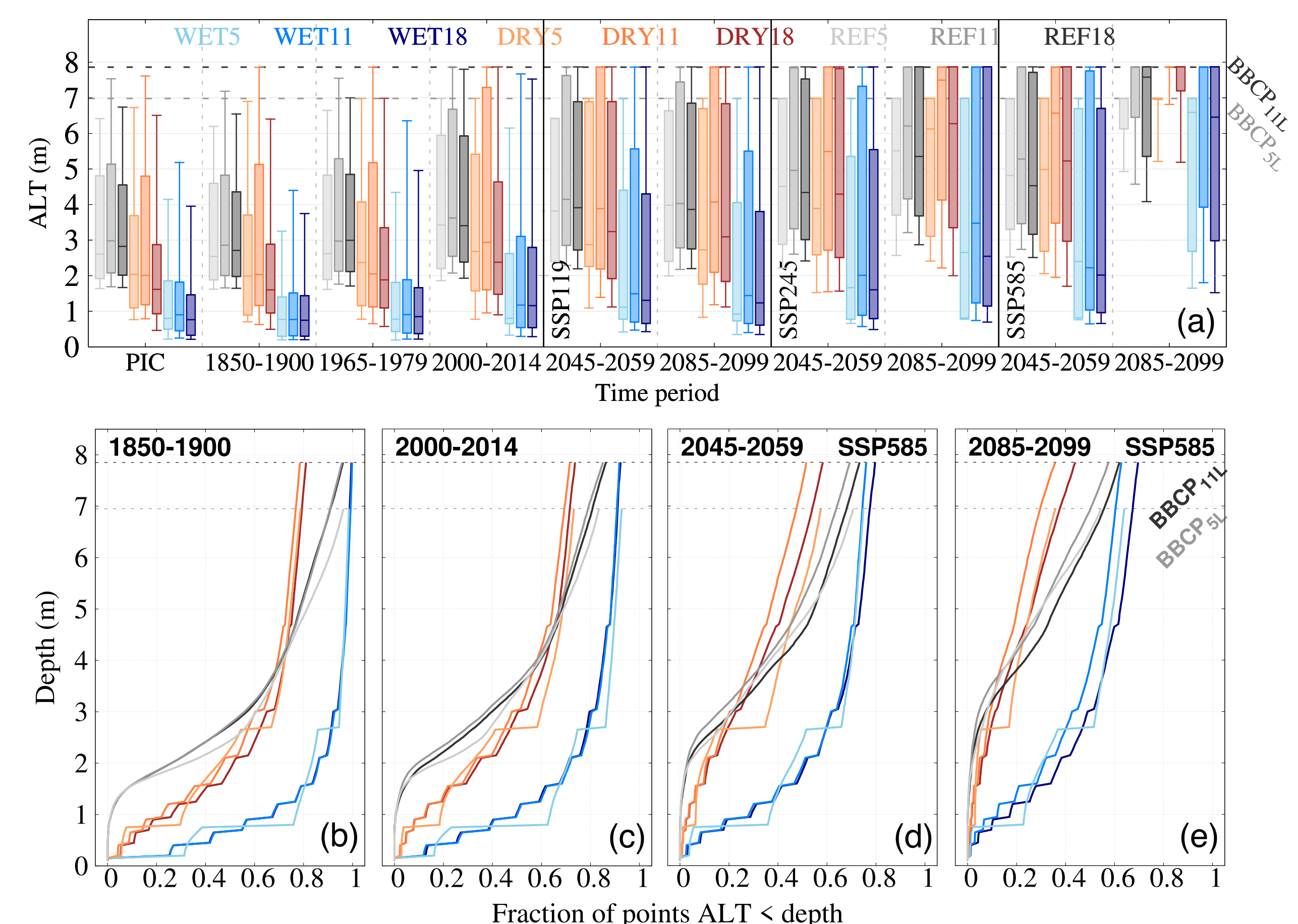


Fig. 3. (a) Spatial distribution of the active layer thickness (ALT, m) for the JSBACH-HTCp ensemble in different periods. Boxplots (whiskers) represent the interquartile (interdecile) ranges for every period and member of the ensemble. (b-e) Fraction of points within the JSBACH-HTCp permafrost mask with an ALT in summer smaller than the indicated depth in the y-axis for different periods. For every plot, dark (light) gray dashed line indicates the LSM depth for the (5-) 11-layer configuration.

3. Permafrost extent (PE): JSBACH-HTCp vs. CMIP6 ensemble

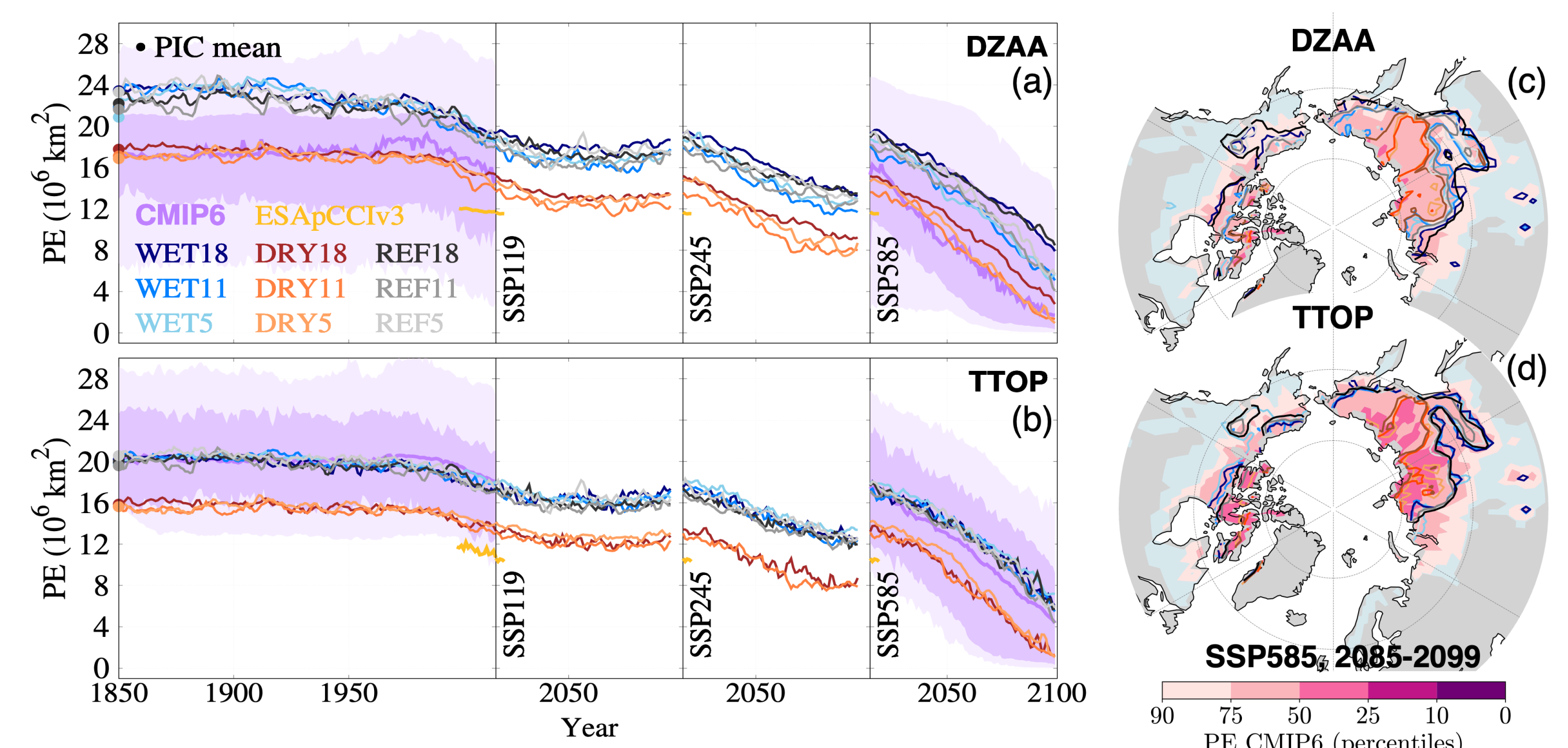
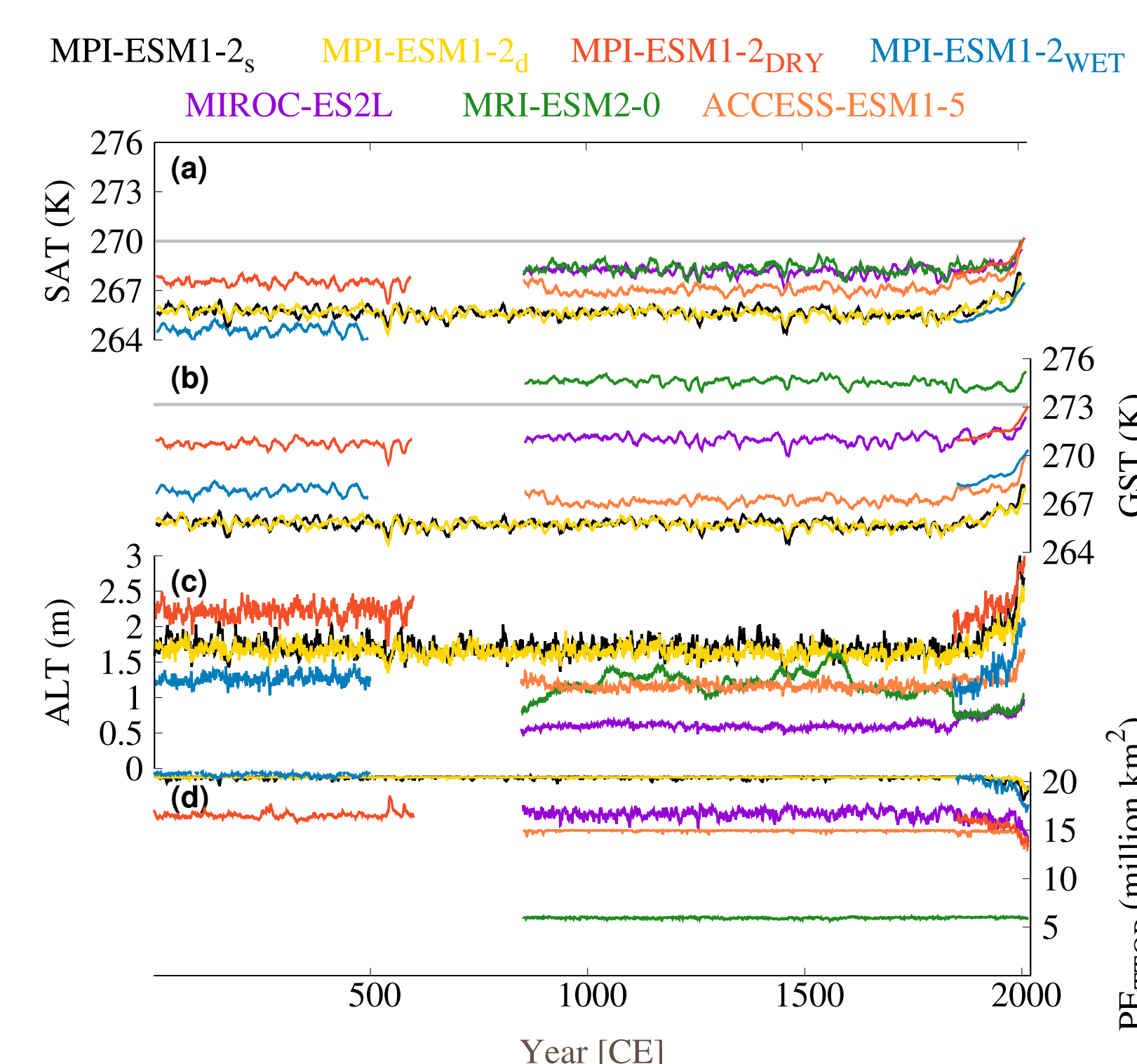


Fig. 4. PE time evolution in the JSBACH-HTCp and CMIP6 ensembles. (Left) PE (in millions of km²) according to DZAA (a) and TTOP (b) permafrost definitions. Lines of different colors (see legend within panel b) indicate the different members of the ensemble, and (light) Navy shading portray the CMIP6 interquartile (P90-P10) range for PE estimates stemming from CMIP6 models given by [9]. (Right) PE maps for JSBACH-HTCp ensemble members (contour lines) and CMIP6 ensemble (filled contours) in 2085-2099 under the SSP585 scenario for DZAA (c) and TTOP (d).

PE is compared in terms of the permafrost area where the subsurface temperatures at the zero-annual amplitude layer (DZAA; Fig. 4a,c) and at the top of the permafrost are greater than 0 °C (TTOP; Fig. 4b,d). Pre-industrial and 20th century DRY (WET) PE is close to CMIP6 median for the DZAA (TTOP) definition. REF yields very similar PE values to WET for both definitions, but with greater variability, which might be linked to the lack of soil water phase changes. **As SSP585 warming intensifies, PE loss is more intense for shallow (5- and 11-) than for deep (18-layer) simulations for TTOP, suggesting a stronger deep-permafrost degradation.**

4. Permafrost response at multi-centennial timescales: the Common Era



In order to characterize the response of permafrost to changes in the hydro-thermodynamics of Arctic soils at centennial and multi-centennial timescales, a couple of JSBACH-HTCp WET18 and DRY18 simulations of the CE are in production.

Fig. 5. Permafrost evolution in the Common Era (CE). Permafrost mean SAT (a), GST (b), ALT (c), and PE according to the TTOP definition (d) in 0-2014 for the four simulations from the PMIP4, a CE simulation performed with a version of the MPI-ESM with a deep LSM [10], and two WET and DRY 18-layer (deep) CE simulations with the JSBACH-HTCp version of the MPI-ESM (in progress). 18-layer WET and DRY JSBACH-HTCp simulations in the historical period are also depicted. The horizontal grey line in (a,b) indicates $T = 0^{\circ}\text{C}$.

The JSBACH-HTCp past2k runs might better depict surface and subsurface temperature, ALT and PE response to volcanic and solar forcings (Fig. 5).

Acknowledgements

We acknowledge the financial support of the Spanish Ministry of Science to GreatModelS (RTI2018-102305-B-C21) and SMILEME (PID2021-126696OB-C21) projects, and funding FGP Ph.D.'s contract (PRE2019-090694). We would also thank the Deutsches Klimarechenzentrum (DKRZ) for the resources its Scientific Steering Committee (WLA) granted to run the JSBACH-HTCp ensemble under project ID bm1026.

References

- [1] Hugelius, G., et al. (2014). **BG**, DOI: 10.5194/bg-11-6573-2014.
- [2] Reick, C. H., et al. (2021). **MPI-M**, DOI: 10.17617/2.3279802.
- [3] de Vrese, P., et al. (2023). **TC**, DOI: 10.5194/tc-17-2095-2023.
- [4] Ekici, A., et al. (2014). **GMD**, DOI: 10.5194/gmd-7-631-2014.
- [5] González-Rouco, J. F., et al. (2021). **JHM**, DOI: 10.1175/JHM-D-21-0024.1.
- [6] Steinert, N. J., et al. (2021). **GRL**, DOI: 10.1029/2021GL094273.
- [7] Melo-Aguilar, C., et al. (2018). **CP**, DOI: 10.5194/cp-14-1583-2018.
- [8] Outcalt, S., et al. (1990). **WRR**, DOI: 10.1029/WR026007p01509.
- [9] Steinert, N. J., et al. (2024). **ERI**, DOI: 10.1088/1748-9326/ad10d7.
- [10] García-Pereira, F., et al. (2024). **ESD**, DOI: 10.5194/esd-15-547-2024.